MJFAS Malaysian Journal of Fundamental and Applied Sciences
ISSN:2289-5981 e-ISSN:2289-599X
UTM UNIVERSITI TEKNOLOGI MALAYSIA

Nitrogen-doped-TiO_2 nanocatalyst for selective photocatalytic CO_2 reduction to fuels in a monolith reactor

Beenish Tahir, Muhammad Tahir, Nor Aishah Saidina Amin*

Chemical Reaction Engineering Group (CREG), Faculty of Chemical and Energy Engineering, Universiti Teknologi Malaysia, 81310 UTM Johor Bahru, Johor, Malaysia.

Corresponding Author: noraishah@cheme.utm.my

Article history :
Received 25 October 2015
Accepted 13 November 2015

GRAPHICAL ABSTRACT

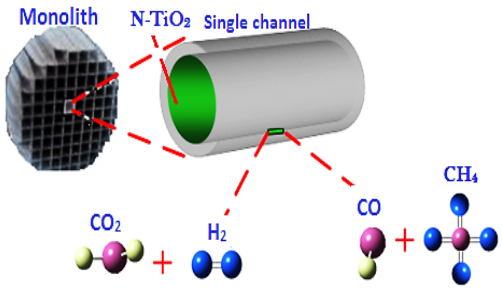

ABSTRACT

In this study, photocatalytic CO_2 reduction with H_2 over nitrogen (N)-doped TiO_2 nanocatalyst in a monolith photoreactor has been investigated. The N-doped TiO_2 nanocatalyst was synthesized by sol-gel method, dip-coated over the monolith channels, and characterized by XRD, SEM and N_2 adsorption-desorption. Highly crystalline and anatase phase TiO_2 was produced in the N-doped TiO_2 samples with increased surface area and reduced crystallite size. The N-doped TiO_2 nanocatalyst demonstrated excellent photoactivity for selective CO_2 reduction to CO in a continuous monolith photoreactor. The 3 wt. % N-doped TiO_2 was found to be the most optimal, giving maximum CO yield rate of 56.30 µmole g-catal.$^{-1}$ h^{-1} with selectivity of 96.3% at CO_2/H_2 feed ratio 1 and feed flow rate 20 mL/min. The performance of monolithic N-doped TiO_2 nanocatalyst for selective and continuous CO production was 4.7 fold higher than un-doped TiO_2. The significantly enhanced TiO_2 activity was evidently due to hindered charges recombination rate due to N-doping. The N-doped TO_2 gave prolonged stability for continuous CO and CH_4 production over the irradiation time.

Keywords: photocatalysis, N-doped TiO_2, greenhouse gas CO_2, H_2 reductant, monolith photoreactor

http://dx.doi.org/10.11113/mjfas.v11n3.379

1. INTRODUCTION

The increasing concentration of greenhouse gas in the atmosphere, in particular CO_2, emitted during fossil fuels combustion is widely accepted as one of the main causes of global warming [1]. Researchers are relentlessly considering various methods to effectively reducing CO_2 concentration. Among the various technologies for CO_2 capture and sequestration, photocatalytic conversion of CO_2 into useful chemicals and fuels is among the prevalent research and gaining significant interests [2-4]. Thus, developing an efficient photocatalysis process seems to be an encouraging technology to alleviate CO_2 emissions and to produce energy bearing compounds.

Among the semiconductor materials, TiO_2 has numerous advantages such as strong oxidative potential, low cost, available in excess, chemically/thermally stable and non-toxic [5,6]. However, the efficiency of TiO_2 is low because of wide band gap (3.20 eV) and immediate recombination of photo-generated electron–hole pairs. Different metals such as Au, Ag, Cu, Ni, and Pt have been investigated to improve TiO_2 photoactivity and selectivity [7-9]. Among the non-metals C, S, F and N are considering as more effective and economical approach to improve TiO_2 photoactivity. However, nitrogen-loaded TiO_2 registered higher photoactivity due to efficient separation of electron-hole (e-/h+) pairs [10,11]. There are limited reports on photocatalytic CO_2 reduction with H_2 over N-doped TiO_2 catalyst. Therefore, it is envisaged that N-doped TiO_2 catalyst would be suitable to enhance CO_2 reduction efficiency via photocatalytic reverse water gas shift reaction.

In photocatalytic CO_2 reduction systems, the type of photoreactor and catalyst support is also vital. The photoreactor is efficient only if it has high ratio of active surface area to reactor volume, efficient light distribution and greater photonic efficiency [12]. Among the structured reactor, monoliths have been exploited for many industrial processes. Its unique structure and high surface area to volume ratio facilitates efficient light harvesting [13,14]. In this study, the N-doped TiO_2 photocatalyst for CO_2 reduction with H_2 in a monolith photoreactor has been investigated for the first time. Therefore, the objective of this study is to test the performance of a monolith photoreactor and N-doped TiO_2 catalyst for selective photocatalytic CO_2 reduction to fuels via reversed water gas shift reaction.

2. EXPERIMENTS

2.1 Catalyst Preparation

Nitrogen doped TiO_2 nanocatalysts were prepared via sol-gel single step method. Typically, 10 mL of titanium tetra-isopropoxide ($Ti(C_3H_7O)_4$) dispersed in 30 mL of isopropanol (C_3H_7O) was hydrolyzed by adding drop wise 7 mL of acetic acid (1M) dissolved in 10 mL isopropanol and stirred for 12 h. Next, an adequate amount of urea dissolved in DI water was added to titanium sol and stirred for another 6 h until a clear sol was produced. The sol obtained was poured into a glass container and was coated over the monolith channels. The amounts of N-doped were 1 to 5 wt. % to the TiO_2 samples. The same procedure was used to prepare TiO_2 nanoparticles.

2.2 Characterization

The crystalline structure of the catalyst was determined with X-ray diffraction (XRD) recorded on a powder diffractometer (Bruker Advance D8, 40 kV, 40 mA) using a Cu Kα radiation source in the range of 2θ = 10-70°. The morphology of the catalysts was observed using scanning electron microscope (SEM) with JEOL JSM6390 LV SEM instrument. The BET analysis of the catalyst was determined by N_2 adsorption-desorption isotherms using a Surfer-Thermo Scientific instrument. The catalyst was degassed at 523 K for 4 h before being subjected to N_2 adsorption, while N_2 adsorption-desorption properties were examined at 77 K. Pore size distributions and pore volumes were determined by means of Barrett-Joyner-Halenda (BJH) method.

2.3 Catalytic Activity Measurements

The CO_2 photoreduction with H_2 was conducted in a continuous monolith photoreactor system [15]. The reactor consisted of a stainless steel cylindrical vessel with total volume 150 cm^3. It is equipped with a quartz window and a reflector lamp located above the reactor. The catalyst coated ceramic monoliths with channels per square inch (CPSI) 100 were inserted in the middle of the reactor chamber. The light source used was a 200W Hg reflector lamp. An optical process monitor ILT OPM-1D and a SED008/W sensor was used to measure the light intensity. Compressed CO_2 and H_2, regulated by mass flow controllers (MFC), were continuously passed through the reactor at feed ratio of CO_2/H_2 1.0 and total flow rates of feed stream 20 mL/min. The products were analyzed using on-line gas chromatograph (GC-Agilent Technologies 6890 N, USA) equipped with a thermal conductivity detector (TCD) and a flame ionized detector (FID).

3. RESULTS AND DISCUSSION

3.1 Characterization of Nanocatalysts

Fig. 1 shows XRD spectra of TiO_2 and N-doped TiO_2 catalysts. XRD peak revealed pure crystalline and anatase phase TiO_2. Similarly, peak of N-doped TiO_2 samples indicated the formation of anatase as the main crystalline phase. The peak attributable to nitrogen is not detected, possibly due to the low amount or it is uniformly distributed over the TiO_2 surface. Similar observations were reported previously [10].

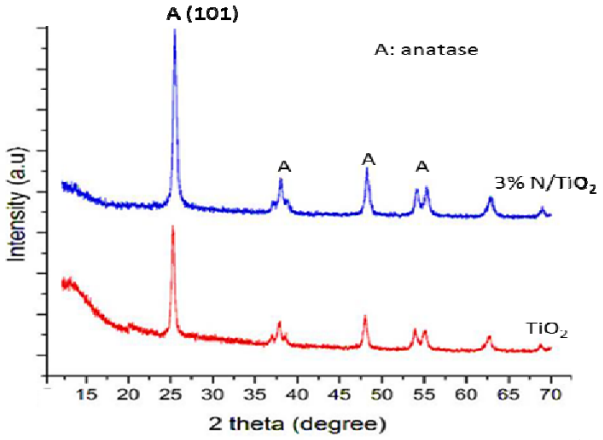

Fig. 1 XRD patterns of TiO_2 and N-doped TiO_2 samples

Fig. 2 depicts SEM micrographs of un-coated and catalyst coated monolith channels to visualize the morphology. Seemingly, all the channels are uniform in size with cordierite structure and square shape as shown in Fig. 2 (a). Fig. 2 (b) revealed uneven and non-uniform channel surface. The catalyst coated monolith channels with uniform and un-broken layer could be seen in Fig. 2 (c). Similarly, Fig. 2 (d) indicates smooth catalyst layer distributed over the monolith channels.

The BET surface area, pore volume and pore diameter is summarized in Table 1. The BET surface area of TiO_2 increased from 43 to 47 m^2/g by N-doping. However, increase in pore volume could be seen in N-doped TiO_2 sample. On the other hand, pore diameter slightly decreased in N-doped TiO_2 sample, possibly N distributed over TiO_2 surface hindered crystal growth.

Table 1 Summary of surface area, pore volume and pore diameter of TiO_2 and N-doped TiO_2 catalysts

Catalyst	BET surface area (m^2/g)	BJH pore volume (cm^3/g)	Pore diameter (nm)
TiO_2	43	0.13	11
3% N/TiO_2	47	0.15	10

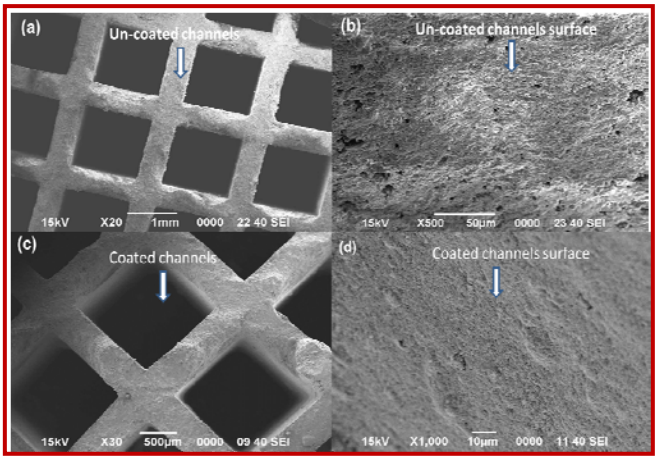

Fig. 2 SEM images of un-coated and catalyst coated monolith channels: (a) bare monolith channels, (b) bare monolith channel surface, (c) catalyst coated monolith channels , (d) catalyst coated channels surface

3.2 Photoactivity test of CO_2 reduction with H_2

Fig. 3 illustrates the effects of different N-doping levels onto TiO_2 photoactivity for CO_2 photoreduction with H_2 to CO and CH_4 under UV-light irradiation in a continuous monolith photoreactor. The un-doped TiO_2 promotes CO production with smaller amount of CH_4 yield but yet poor photoactivity is registered. The N-doping into TiO_2 effectively promotes the formation of CO, the main product detected in gaseous mixture with appreciable amount of CH_4, over all the N-doped TiO_2 samples. The CO production increased remarkably with N-doping up to an optimum 3wt. % N-content, and then gradually decreased. Therefore, 3 wt. % N doped TiO_2 is the most effective over which amount of evolved CO reached to 178 µmole g-catal.$^{-1}$ after 2h of irradiation time, which was significantly higher than the un-doped TiO_2 (38 µmole g-catal.$^{-1}$). The higher yield of CO confirms hindered charges recombination rate by N-doping.

Fig. 4 illustrates dynamic CH_4 production as a function of irradiation time over un-doped TiO_2 and 3 wt. % N-doped TiO_2 monolithic catalysts. Evidently, the amount of CH_4 gradually increased with the irradiation time over N-doped TiO_2 catalysts. However, TiO_2 catalyst lost its photoactivity after 5h of irradiation time. This revealed prolonged stability of N-doped TiO_2 catalyst for continuous CH_4 production in a monolith photoreactor. The yield of CH_4 over N-doped TiO_2 was 3.3 fold higher than pure TiO_2 monolithic catalyst, confirming N-metal serves as an efficient charges separation doped in TiO_2 catalyst for CO_2 photo-reduction to CH_4.

The yield of CO production via CO_2 reduction over TiO_2 and N-doped TiO_2 at different irradiation times is presented in Fig. 5. Initially, the yield of CO production is much faster, but gradually decreased after 4 h of irradiation time over both catalysts. The amount of CO produced over 3 wt. % N-doped TiO_2 monolithic catalyst was 225 µmole g-catal.$^{-1}$, significantly high than the un-doped TiO_2. The much higher photoactivity confirms the potential of CO_2 reduction with H_2 in monolith photoreactor. At prolonged irradiation times, CO production decreased over both catalysts, possibly due to decrease in catalysts photoactivity in continuous operation of monolith photoreactor. However, N-doped TiO_2 catalyst found more stable than TiO_2, confirming N-doped into TiO_2 provides both activity and photostability.

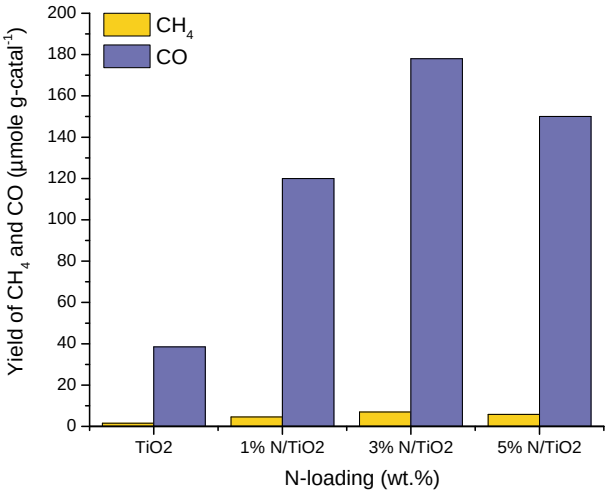

Fig. 3 Effect of N-loading on TiO_2 photoactivity for CO_2 reduction with H_2 for irradiation time 2h, CO_2/H_2 ratio 1.0 and feed flow rate 20 mL/min

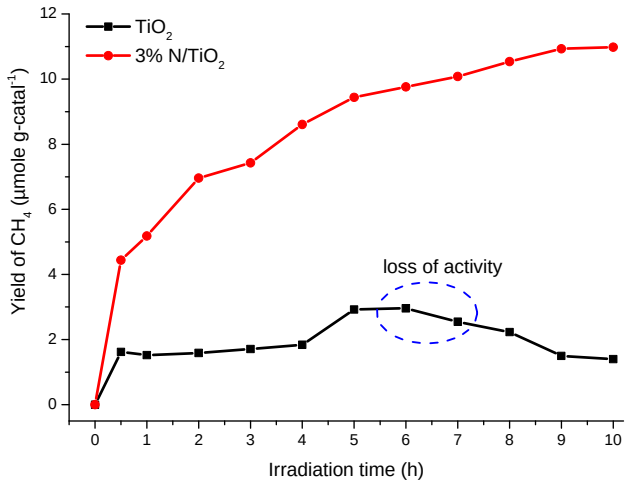

Fig. 4 Effect of irradiation time on CO_2 photoreduction with H_2 to CH_4over TiO_2 and N/TiO_2 catalyst in continuous monolith photoreactor at CO_2/H_2 ratio 1.0 and feed flow rate 20 mL/min

Table 2 summarizes yield rates and selectivity of different products over TiO_2 and N-doped TiO_2 catalysts during photocatalytic CO_2 reduction with H_2. The products observed were CO and CH_4 with traces of C_2H_4 and C_2H_6 over N-dopedTiO_2 monolithic catalysts. The photoactivity

for CO production over N-doped TiO_2 was 56.12 µmole g-catal.$^{-1}$ h^{-1} which was 4.7 fold high than un-doped TiO_2. The selectivity of CO production over TiO_2 and N-doped TiO_2 were much closer, about to 96 %. Recently, N-doped TiO_2 catalyst has been reported for CH_3OH production with yield rate of 23 µmole g-catal.$^{-1}$ h^{-1} in a batch mode operation of photoreactor. [11]. Similarly, g-C_3N_4-N-TiO_2 hetero-junction was tested for CO_2 reduction with H_2O to CO with maximum yield of 14.73 µmole after 12 h irradiation time in batch mode operation [16]. Therefore, the role of N is prominent and much higher CO production was conceivably due to efficient separation of charges by N-metal and obviously due to a larger illuminated surface area with higher photon energy consumption over monolith channels [17].

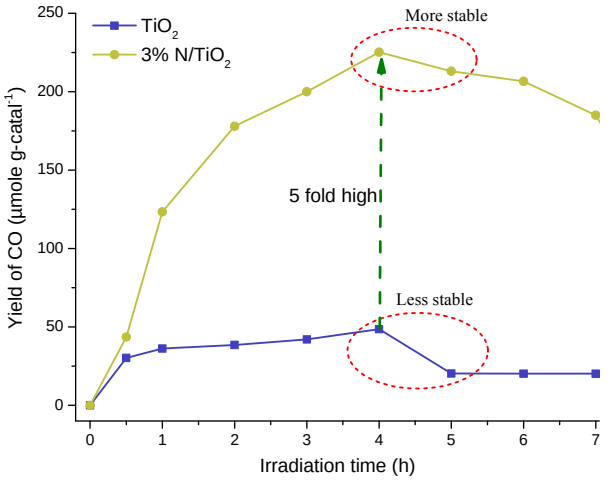

Fig. 5 Selective CO_2 photoreduction to CO over N/TiO_2 at different irradiation time in a continuous monolith photoreactor using CO_2/H_2 ratio 1.0 and feed flow rate 20 mL/min.

Table 2 Summary of yield rates and selectivity of products during CO_2 reduction with H_2 over TiO_2 and N-doped TiO_2 catalysts

Catalyst	Yield rate (µmole g.catal.$^{-1}$ h^{-1})		Selectivity (%)	
	CO	CH_4	CO	CH_4
TiO_2	12.12	0.46	96.34	3.65
3% N/TiO_2	56.30	2.15	96.32	3.68

4. CONCLUSION

The N-doped TiO_2 monolithic nanocatalysts were tested for continuous CO_2 reduction with H_2 in a monolith photoreactor. CO and CH_4 were observed as the main products during CO_2 reduction. The photoactivity of N-doped TiO_2 was 4.7 fold greater than pure TiO_2 with selectivity 96 % at CO_2/H_2 mole ratio 1.0, and feed flow rate 20 mL/min. The N-doped TiO_2 was very stable for CH_4 production while its photoactivity gradually reduced for CO production after 4 h of irradiation time. On the other hand, a lower stability of TiO_2 catalyst observed for both CO and CH_4 production. The higher efficiency of N-doped TiO_2 and monolith photoreactor was obviously due to a larger illuminated surface area, higher photon energy consumption and better charges separation by N-element.

ACKNOWLEDGEMENTS

The authors would like to extend their deepest appreciation to MOHE and Universiti Teknologi Malaysia for the financial support under Vot 02G14 and Vot 4F404.

REFERENCES

[1] M. Tahir, N.S. Amin, Renewable Sustainable Energy Rev. 25 (2013) 560.
[2] Z. Li, Y. Zhou, J. Zhang, W. Tu, Q. Liu, T. Yu, Z. Zou, Crystal Growth & Design 12 (2012) 1476.
[3] E. Liu, L. Qi, J. Bian, Y. Chen, X. Hu, J. Fan, H. Liu, C. Zhu, Q. Wang, Mater. Res. Bull. 68 (2015) 203.
[4] M. Tahir, N.S. Amin, Appl. Catal., B: Environ. 142-143 (2013) 512.
[5] R. Sasikala, A.R. Shirole, V. Sudarsan, Jagannath, C. Sudakar, R. Naik, R. Rao, S.R. Bharadwaj, Appl. Catal. A: Gen. 377 (2010) 47.
[6] L. Liu, F. Gao, H. Zhao, Y. Li, Appl. Catal., B: Environ. 134-135 (2013) 349.
[7] D. Kong, J.Z.Y. Tan, F. Yang, J. Zeng, X. Zhang, Appl. Surf. Sci. 277 (2013) 105.
[8] B.S. Kwak, K. Vignesh, N.-K. Park, H.-J. Ryu, J.-I. Baek, M. Kang, Fuel 143 (2015) 570.
[9] Z. Xiong, H. Wang, N. Xu, H. Li, B. Fang, Y. Zhao, J. Zhang, C. Zheng, Int. J. Hydrogen Energ. 40 (2015) 10049.
[10] X. Li, Z. Zhuang, W. Li, H. Pan, Appl. Catal. A: Gen. 429-430 (2012) 31.
[11] B. Michalkiewicz, J. Majewska, G. Kądziołka, K. Bubacz, S. Mozia, A.W. Morawski, Journal of CO_2 Utilization 5 (2014) 47.
[12] K. Yuan, L. Yang, X. Du, Y. Yang, Energy Convers. Manage. 81 (2014) 98.
[13] M. Tahir, N.S. Amin, Chem. Eng. J. 230 (2013). 314.
[14] P.-Y. Liou, S.-C. Chen, J.C.S. Wu, D. Liu, S. Mackintosh, M. Maroto-Valer, R. Linforth, Energy Environ. Sci. 4 (2011) 1487.
[15] M. Tahir, B. Tahir, N.S. Amin, Mater. Res. Bull. 63 (2015) 13.
[16] S. Zhou, Y. Liu, J. Li, Y. Wang, G. Jiang, Z. Zhao, D. Wang, A. Duan, J. Liu, Y. Wei, Appl. Catal., B: Environ. 158–159 (2014) 20.
[17] B. Tahir, M. Tahir, N.S. Amin, Energy Convers. Manage. 90 (2015) 272.